Optical vibrational modes of ZnSe-ZnS_xSe_{1-x} strained-layer superlattices

D. J. Olego, K. Shahzad, D. A. Cammack, and H. Cornelissen*
Philips Laboratories, North American Philips Corporation, 345 Scarborough Road, Briarcliff Manor, New York 10510
(Received 11 March 1988)

Resonant-Raman-scattering experiments were carried out at low temperatures to study the optical lattice modes of ZnSe-ZnS_xSe_{1-x} strained-layer superlattices, which were grown by molecular-beam epitaxy on (100) surfaces of GaAs substrates. The observed Raman modes can be classified into two groups: One group corresponds to vibrations with amplitudes localized either in the ZnSe or in the ZnS_xSe_{1-x} layers. These are the confined modes. In the second group, the phonons with amplitudes in both layers are included, namely, interface vibrations and folded optical modes. The measured dependence of the confined and delocalized phonons on sample parameters (individual layer thicknesses, superlattice period, total superlattice thickness, and interfacial strain) and on resonant excitation is presented and discussed in detail. The trends that were established are compared with the theoretical predictions of lattice-dynamic models for multilayer structures. Experimental data on the lattice-dynamic properties of ZnS_xSe_{1-x} alloys are included for comparison purposes and to unequivocally distinguish superlattice effects. These data were gathered with ternary layers grown and measured under similar conditions as the superlattices. Concomitant with vibrational characteristics, this work has also yielded an insight into other intrinsic properties of strained-layer superlattices. The interplay between confinement and strain in the renormalization of phonon frequencies was elucidated from an experimental point of view and this information was applied to characterize the nature of the superlattice transition from pseudomorphic to free standing.

I. INTRODUCTION

The vibrational properties of semiconductor superlattices have recently been given considerable attention. Various experimental and theoretical papers have elucidated the nature of the phonon modes in superlattices and the manner in which they depend on the artificial periodicity induced by the alternating stacking of individual layers.[1] For modes with wave vectors **q** perpendicular to the layers (the z direction), folded and confined phonons have been identified. The folded modes propagate through the entire superlattice with **q** allowed in a zone determined by the inverse of the superlattice period. These modes fall in the frequency regions for which a substantial overlap exists in the phonon density of states of the bulk semiconductors that form the superlattice. One of these regions comprises the acoustical frequencies. On the other hand, the confined modes are localized in one type of layers of the superlattice with negligible penetration in the contiguous layers. They form patterns that in first order resemble the standing waves of isolated slabs with zone edge **q** inversely proportional to the thickness of the layers in which the modes are found. The confined modes have frequencies in the optical spectral range. For the modes that propagate with **q** parallel to the layer surfaces (the x,y directions), besides the extra periodicity of the superlattice the dielectric properties of the layers play a role in determining the nature and frequencies of the vibrations. For example, the so-called interface modes arise because of the dielectric discontinuity at the interfaces between the layers. These modes have maximum peak amplitude at the interfaces but they display some field penetration on both sides of them. In addition to the effects mentioned above, if there is a lattice mismatch between the individual bulk semiconductors that form the superlattice one has to consider the effects of elastic strains on the phonon frequencies. This is particularly important for the confined modes because in most of the cases they are almost dispersionless.

Raman scattering is widely used as the experimental probe to study lattice vibrations in superlattices. The **q** transfer induced in a first-order Raman process is negligibly small compared with the edges of the Brillouin zone of bulk semiconductors. However, in superlattices because of the zone folding, the **q** of the Raman modes is comparable to the full extent of the minizone. Hence, mapping of phonon dispersions and measurements of minigap openings can be done. By matching the energy of the laser excitation to electronic transitions one can selectively enhance the modes of one of the layers of the superlattices thus achieving spatial resolution. The technique provides also the capability of measuring frequency shifts with accuracies of tenths of an inverse centimeter, which makes strain determinations straightforward and nondestructive.

This paper deals with the properties of the optical phonons of ZnSe-ZnS_xSe_{1-x} strained-layer superlattices (SLS), which were investigated with Raman spectroscopy. There is much current interest in ZnSe-based structures from fundamental and applied points of view. The vibrational properties of two such systems have been investigated so far, namely, ZnSe-$Zn_{1-x}Mn_xSe$ and ZnSe-ZnTe superlattices.[2,3] Most of the work has emphasized the effects of strain on the optical phonons. In the case of ZnSe-ZnS_xSe_{1-x} superlattices, in addition to ascertaining strain related effects, we also report here the observation

of confined optical modes in the ZnSe layers, interface modes, and additional modes in the frequency range of the vibrations of ZnS_xSe_{1-x}. The latter are tentatively assigned to folded or delocalized optical phonons.

The sample parameters of the investigated superlattices are given in Table I. For the values of composition x of the ternary ZnS_xSe_{1-x} layers, the lattice mismatch between ZnSe and ZnS_xSe_{1-x} given by $f=2(a_{ZnSe}-a_{ZnS_xSe_{1-x}})/(a_{ZnSe}+a_{ZnS_xSe_{1-x}})$ can be as large as 0.01. This mismatch is the source of compressive strains in the ZnSe layers and tensile ones in the ternary ZnS_xSe_{1-x} layers. The compressive strain will induce a blue shift in the longitudinal-optical (LO) frequency of ZnSe that counterbalances the expected red shift due to confinement. Therefore, in order to separate the effects of confinement from those of strain we have devised some samples in which the composition x and the individual layer thicknesses d_{ZnSe} and $d_{ZnS_xSe_{1-x}}$ or their ratios $d_{ZnSe}/d_{ZnS_xSe_{1-x}}$ are kept almost constant from sample to sample and only the total superlattice thicknesses D are changed. Red shifts due to confinement are measured for the LO phonons of the ZnSe layers in the thinnest superlattices. With increasing D a continuous buildup of the strain in the ZnSe layers is observed, which is taken as an indication of a gradual transition from the congruent to the free-standing state in ZnSe-ZnS_xSe_{1-x} superlattices. In the set of samples described in Table I we also have a reasonably large variation of the superlattice period $d=d_{ZnSe}+d_{ZnS_xSe_{1-x}}$ which provides an additional degree of freedom in this study.

To identify unequivocally interface modes in a ternary-binary superlattice and in our particular case to establish the origin of the extra modes seen at the ZnS_xSe_{1-x} frequencies, we had to pay attention to the vibrational properties of the ternary alloy itself. For this reason we have studied and included in this paper Raman data of ZnS_xSe_{1-x} alloy samples which were grown and measured under similar conditions as the superlattices. Multiphonon scattering detected under different resonant conditions has contributed also to the characterization of the nature of the phonon modes in the superlattices. The energy gaps of ZnSe and ZnS_xSe_{1-x} lie in the deep blue spectral region above 2.7 eV. These energies are difficult to reach with tunable laser sources for resonant excitation. Therefore, we tuned x in the samples of Table I to obtain resonant conditions to discrete laser lines.

TABLE I. Parameters of the ZnSe-ZnS_xSe_{1-x} strained-layer superlattices used in this study. The individual thicknesses of the ZnSe and ZnS_xSe_{1-x} layers are given in angstroms by d_{ZnSe} and $d_{ZnS_xSe_{1-x}}$, respectively. The total superlattice thickness is represented by D in the units of μm. The composition of the ternary layers is given by x.

Sample No.	d_{ZnSe} (Å)	$d_{ZnS_xSe_{1-x}}$ (Å)	D (μm)	x
1	40	43	0.1	0.2
2	41	45	0.3	0.2
3	40	40	0.55	0.2
4	46	49	0.88	0.21
5	20	24	1.0	0.25
6	55	66	4.3	0.18
7	30	128	1.0	0.29
8	25	38	0.15	0.2
9	18	25	0.15	0.2

The organization of the paper is as follows. Section II describes the growth of the samples, the characterization of their parameters, and how the Raman measurements were performed. Section III deals with the vibrational properties of ZnS_xSe_{1-x} and the expected frequency ranges in which confined, folded, and interface phonons should be seen. In Sec. IV the dependence of the longitudinal-optical frequencies of ZnSe on $\mathbf{q}$ and strain is reviewed. The background material developed in Secs. III and IV is used in the discussions of the experimental results which are presented in Sec. V. Finally, a summary of the work is given in Sec. VI.

II. EXPERIMENTAL

The ZnSe-ZnS_xSe_{1-x} superlattices were grown by molecular-beam epitaxy with polycrystalline charges of ZnSe and $ZnS_{0.5}Se_{0.5}$ as the sources of the molecular beams. GaAs wafers with (001) surfaces were used as substrates. The substrate temperature during growth was kept at $\approx$350 °C and typical growth rates were in the range of 0.5 μm/h. To minimize effects due to the mismatch with the substrate all the superlattices were grown on a micrometer-thick ZnSe buffer layer deposited *in situ* on the GaAs surface. At this thickness high-quality ZnSe is obtained and the strain induced by the mismatch with the substrate is completely relaxed.[4]

The layer thicknesses d_{ZnSe} or $d_{ZnS_xSe_{1-x}}$ were measured by transmission-electron microscopy and the total superlattice thickness D was determined either with scanning or transmission-electron microscopy and was corroborated by the growth parameters. Pictures of the superlattices taken with transmission-electron microscopy reveal very sharp interfaces between the alternating layers. The composition of the ternary layers in the superlattices was established with Raman scattering by using the dependence of the optical modes of ZnS_xSe_{1-x} on x measured independently with the samples described below. In some superlattices photoluminescence from the ZnS_xSe_{1-x} layers was detected and also used to determine x. An excellent agreement was found between the Raman and photoluminescence values of x. The control ZnS_xSe_{1-x} layers with typical thicknesses above 1.5 μm were grown following the same procedure just outlined. Their composition was established with an accuracy better than 2% with energy-dispersive analysis of x rays.

The Raman measurements were performed in backscattering geometry with the incident photons along the $\langle 001 \rangle$ directions and with the incoming and outgoing polarizations lying along the $\langle 110 \rangle$ directions. The scattering geometry is described by the standard notation $z(x+y,x+y)\bar{z}$. The excitation was provided by a Kr^+-ion laser operating at 4131 Å. The penetration depth of the laser photons is $\approx$1000 Å and therefore the Raman signal is representative of several periods.[5] The

Raman scattered light was analyzed in frequency by a computer-controlled wavelength-driven double monochromator and photon-counting electronics was used for detection. During the recording of the Raman spectra the samples were mounted in a cold finger of a closed-cycle cryostat and cooled down to ≈ 12 K. The energy of the laser photons lie between 100 and 150 meV above the fundamental edge of the superlattices in the ZnSe wells. The absorption edge of the ZnS_xSe_{1-x} layers, for $x \approx 0.2$ is slightly above the energy of the incoming photons. In the case of sample 6 the ternary band gap is ≈ 90 meV below the photon energy and therefore we will have resonant conditions with the superlattice fundamental gap and with states in the ZnS_xSe_{1-x} barriers as well.

III. OPTICAL PHONONS OF ZnS_xSe_{1-x}: IMPLICATIONS FOR SUPERLATTICE MODES

Figure 1 shows the low-temperature first-order Raman spectra of molecular-beam epitaxy grown layers of ZnS_xSe_{1-x} for chosen values of the composition x. The peaks labeled LO_1 and LO_2, which are seen in the spectra of all ZnS_xSe_{1-x} alloy samples, are attributed to $\mathbf{q} \approx 0$ LO phonons. The selection rules for scattering from (001) surfaces predict the creation of LO modes in the Raman process.[6] In some samples, two other weaker structures identified as TO_1 and TO_2 in Fig. 1 are detected. Their origin is ascribed to $\mathbf{q} \approx 0$ transverse-optical (TO) modes and their appearance in the spectra from (001) surfaces is explained in terms of breakdown of $\mathbf{q}$ conservation in the scattering process due to alloy disorder or slight misorientation in the samples. The (LO_1,TO_1) pair corresponds to ZnSe-like vibrations and the other pair (LO_2,TO_2) to ZnS-like ones. The presence of two distinct sets of vibrations in the layers confirms previous reports that ZnS_xSe_{1-x} displays a two-mode behavior.[7] The full compositional dependence of the LO_i and TO_i ($i=1$ and 2) Raman peaks is shown in Fig. 2. The LO modes display a stronger dependence on x than the TO ones and in particular we can see that the LO_2 frequencies are very sensitive to x in the range of compositions of the ternary layers of the superlattices described in Table I. Therefore, the LO_2 frequencies can be used to rapidly gauge x in the superlattices. For further discussions it is important to mention that in the spectra shown in Fig. 1 and also for all the other ternary samples investigated no additional features are seen between the LO_1 and TO_1 peaks and between the LO_2 and TO_2 peaks.

The two-mode nature of the vibrations of ZnS_xSe_{1-x} has implications for the lattice-dynamic properties of the superlattices.[1] We can see in Fig. 2 that a large frequency gap exists between the LO_2 modes of ZnS_xSe_{1-x} and the LO phonon of ZnSe (LO_{ZnSe}). The LO_{ZnSe} frequency corresponds to the LO_1 frequency for $x=0$. Similarly for

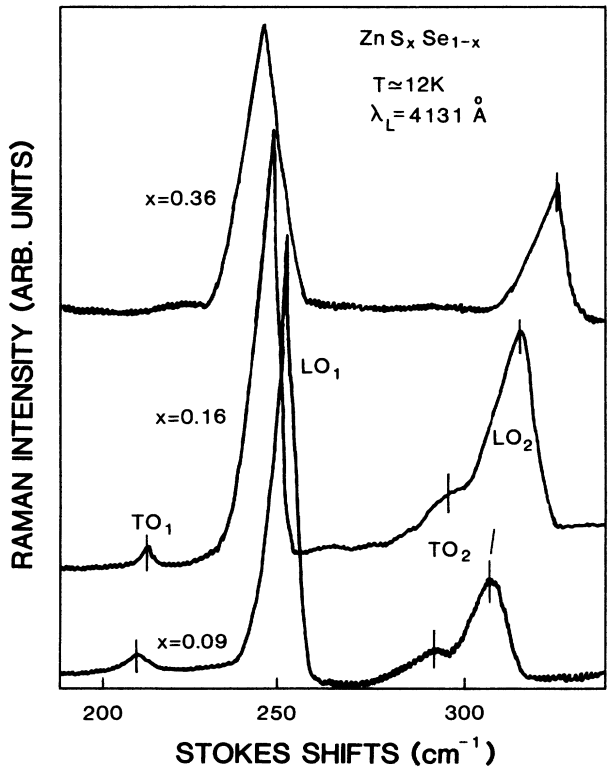

FIG. 1. Stokes first-order Raman spectra of ZnS_xSe_{1-x} layers of various compositions x grown by molecular-beam epitaxy on GaAs substrates. A two-mode behavior is displayed by the optical phonons of these layers. The LO_1 and TO_1 peaks correspond to ZnSe-like vibrations and the LO_2 and TO_2 peaks to ZnS ones.

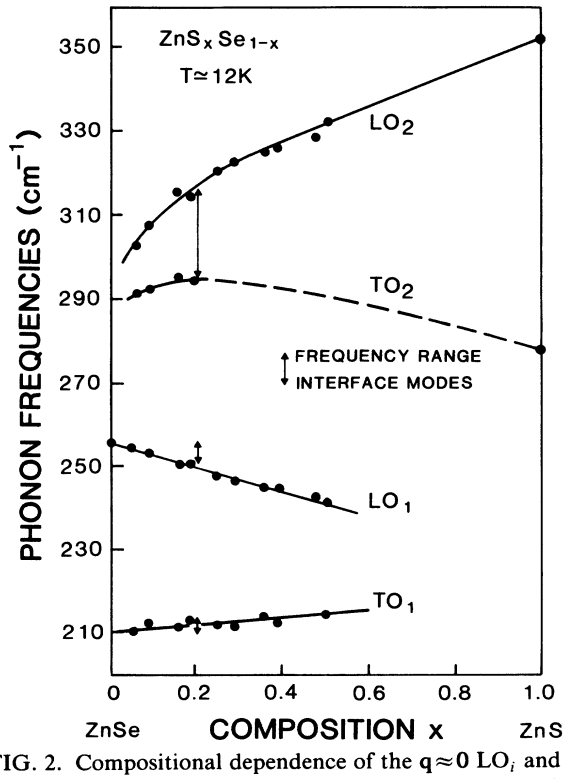

FIG. 2. Compositional dependence of the $\mathbf{q} \approx 0$ LO_i and TO_i frequencies determined from the peak positions measured in the Raman spectra of the ternary layers. The solid and dashed lines are drawn through the experimental points as visual aids. The arrows indicate the frequency ranges at which interface modes can be expected in ZnSe-ZnS_xSe_{1-x} strained-layer superlattices for the case of $x=0.2$.

$\mathbf{q}\approx 0$ and fixed $x\neq 0$, there is a frequency difference between LO_{ZnSe} and $LO_1(x)$. Therefore, in a ZnSe-ZnS_xSe_{1-x} superlattice the long wavelength LO_2 and LO_{ZnSe} phonons are expected to give rise to confined modes in the ternary and binary layers, respectively. On the other hand, if one considers $\mathbf{q}$ dispersion, the LO_{ZnSe} frequencies and the LO_1 will overlap, which in turn opens the possibility for modes with LO_1 character to propagate through the ZnSe layers with little attenuation.

With respect to the interface modes, they are expected in the frequency ranges for which the ratio $\eta(\omega)$ of the dielectric constants $\epsilon_{ZnSe}(\omega)/\epsilon_{ZnS_xSe_{1-x}}(\omega)$ is negative.[1,8,9] In the approximation that $\epsilon_i(\omega)$ at the optical frequencies can be represented by that of a collection of oscillators, $\eta(\omega)$ turns out to be negative between TO_{ZnSe} and TO_1, between LO_1 and LO_{ZnSe}, and between TO_2 and LO_2. These frequency ranges are depicted by the arrows of Fig. 2 for a typical value of $x=0.2$. With the exception of the region between the TO_2 and LO_2 frequencies, the other two frequency spans for interface modes are very narrow.

IV. DISPERSION AND STRAIN DEPENDENCE OF LO_{ZnSe} FREQUENCIES; IMPLICATIONS FOR CONFINED MODES

It has been shown that in the absence of strain, the frequency ω_n of the n confined optical mode in layer i can be estimated from the bulk phonon dispersion $\omega(\mathbf{q})$ in which $|\mathbf{q}|=q$ is replaced by $q_n=(na_i)/(2d_i+a_i)$, where a_i is the lattice constant and d_i represents the thickness of the layer.[10] An analytical expression for the bulk dispersion $\omega(\mathbf{q})$ can be obtained with linear chain models either by selecting specific experimental frequency values as input parameters or by fitting the entire experimental $\omega(\mathbf{q})$ measured with neutron scattering. To analyze the case of the LO vibrations of the ZnSe layers, we used the second approach and fitted the published neutron scattering data for $\mathbf{q}\|[001]$ in Ref. 11 to the expression $\omega^2(q)=A+\{A^2-B[1-\cos(\pi q)]\}^{1/2}$,[12] with q in units of $2\pi/a_{ZnSe}$ and ranging from 0 to 1. The LO_{ZnSe} value of Fig. 2 is given by $\omega(0)$ in the expression just mentioned. Figure 3 shows the experimental data reported in Ref. 11 and our fitting results which were obtained with the parameters $A=3.2\times 10^4$ cm^{-2} and $B=4.5\times 10^8$ cm^{-4}. The solid curve gives the calculated frequencies and the agreement with the experimental values is rather good with the exception of $\mathbf{q}$ closer to zone edge. Even more sophisticated models fail to reproduce the measured values in this range of q. We anticipate that the largest magnitude of q needed to explain the superlattice results lies below 0.4, which is a region well described by the analytical expression.

Because of the negative curvature of $\omega(q)$, confinement will push the LO frequencies in the ZnSe layers towards smaller values rather than the $\mathbf{q}=0$ of the bulk. To have a feeling of the magnitude of the effect, we have evaluated the red shifts $\omega_n-\omega(0)$ as a function of d_{ZnSe} with the dispersion relation and q_n described above. The results are represented by the solid lines in Fig. 4 for the first

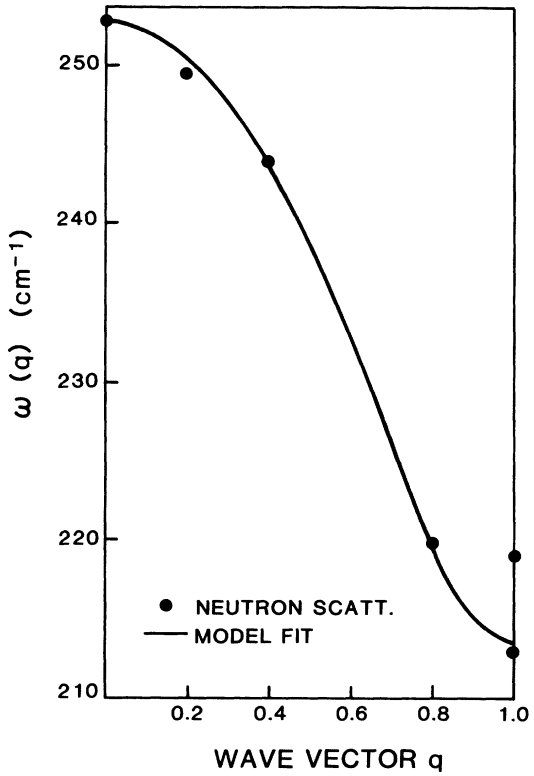

FIG. 3. Wave-vector dispersion of the longitudinal-optical phonons of ZnSe between Γ and X. The magnitude of the wave vector is given by multiplying q by $(2\pi/a_{ZnSe})$. The dots are the measured frequencies with neutron scattering reproduced from Ref. 11. The solid line is a model fit to the experimental values obtained with the expression and parameters given in Sec. IV.

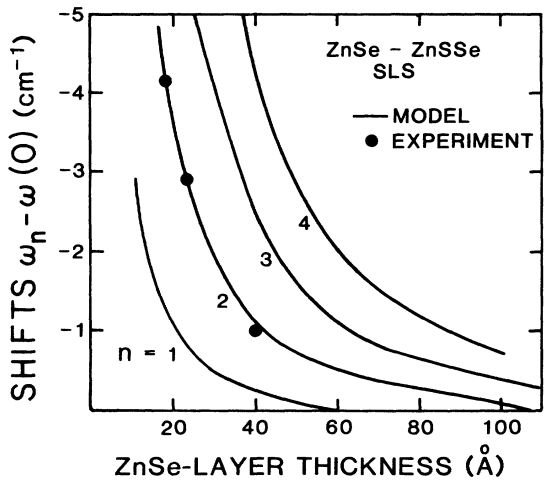

FIG. 4. Shifts of the longitudinal-optical frequencies of confined modes in the ZnSe layers with respect to the $\mathbf{q}=0$ value in the bulk, as a function of layer thickness. The solid lines are the estimated shifts based on the $\omega(q)$ dispersion described in Sec. IV. The dots are the measured values for the strain-free ZnSe layers of the thinnest superlattices (samples 1, 8, and 9).

four confined modes. In the case of $n=1$ or 2, the shifts are smaller for almost all values of d_{ZnSe} than the so-called LO_1-LO_{ZnSe} "phonon barrier." This barrier is on the order of 6 cm^{-1} for x in the neighborhood of 0.2. Therefore the confinement model is valid for these modes. We also note that for $d_{ZnSe} > 40$ Å the shifts due to confinement are very small in absolute values. On the other hand, the shifts corresponding to the $n > 2$ modes become comparable to the phonon barrier for $d_{ZnSe} \leq 30$ Å. These modes will be much less confined in the ZnSe layers because they overlap with the LO_1 vibrations.

If the ZnSe-ZnS_xSe_{1-x} superlattices are not congruent with the ZnSe buffer layer, the lattice mismatch f between ZnSe and ZnS_xSe_{1-x} will give rise to a tetragonal distortion of the ZnSe unit cell. The distortion comes about because of compressive strains along x and y induced by the smaller lattice constant of ZnS_xSe_{1-x}. The built-in strain induces shifts in LO_{ZnSe} which have already been discussed in great detail in the literature.[13] These shifts are described by the expression $\Delta\omega(\epsilon)=421.14\epsilon$ where $\epsilon=\epsilon_{xx}=\epsilon_{yy}$ represents the magnitude of the strain.[13,14] The convention adopted here is that ϵ is positive for compressive strains, which means that LO_{ZnSe} increases under compression. Therefore in the superlattices, the shifts in LO_{ZnSe} induced by the strains are of opposite sign from those due to the confinement. In addition, the strain can very easily determine the frequency values of the LO modes. As an example we estimate that for a moderate strain of $\epsilon=0.0025$ (which corresponds roughly to one-fourth of f), LO_{ZnSe} will shift to higher frequencies by about 1 cm^{-1}. This shift is larger than the one induced by confinement for $n \leq 2$ and d_{ZnSe} above 40 Å. Given the fact that in the Raman spectra the strongest modes are usually the $n=1$ or 2, it becomes evident that to ascertain confinement effects one has to deal with very thin and strain-free ZnSe layers. We will show that this is the case in samples 1, 8, and 9.

V. RESULTS AND DISCUSSIONS

Figure 5 displays the first-order Stokes Raman spectra for some of the ZnSe-ZnS_xSe_{1-x} superlattices listed in Table I. These spectra are typical examples of the kind of Raman data obtained for all the SLS samples studied. We can see that the spectra consist of several structures some of which can be readily identified in light of the results presented in Figs. 1 and 2. For instance, the peaks labeled LO_1, TO_2, and LO_2 are related to vibrational modes of the ZnS_xSe_{1-x} layers and the LO_{ZnSe} peaks are due to ZnSe phonons. On the other hand, there are other Raman bands in Fig. 5 such as I_i and F which appear only in the superlattice case and do not have their counterparts in the spectra of binary or ternary samples. The overall behavior of the Raman modes observed in Fig. 5 and in the spectra of the other samples in Table I can be summarized as follows: the LO_{ZnSe} peaks, which are always the sharpest ones, have frequencies that depend on both the ZnSe-layer thickness d_{ZnSe} and on the total superlattice thickness D. The frequencies of the $LO_{1,2}$ peaks are more sensitive to x than to other superlattice parameters. The I_i bands appear roughly at the same frequency positions in almost all the samples. The I_2 band shows up in many superlattices as a shoulder to the low-energy side of the LO_{ZnSe} peak and the TO_1/I_1 mode is not always observed. Finally, the appearance of the bands labeled F seems to depend on the superlattice period d. Based on the observations just described and other arguments to be put forward in the next paragraphs we ascribed these origins to the Raman modes of the superlattices: LO_{ZnSe} and LO_2 correspond to confined LO vibrations in the ZnSe and ZnS_xSe_{1-x} layers respectively; LO_1 and F are due to delocalized LO phonons; I_i are produced by interface modes, and TO_i arise from TO vibrations of ZnS_xSe_{1-x}.

The Raman spectra shown in Fig. 5 were taken under the resonant conditions described in Sec. II and in the geometry $z(x+y,x+y)\bar{z}$ for polarized scattering. The selection rules allow LO-like modes of A_1 and B_2 symmetries belonging to the D_{2d} point group of the superlattices grown along z.[6,10] The A_1 phonons scatter through

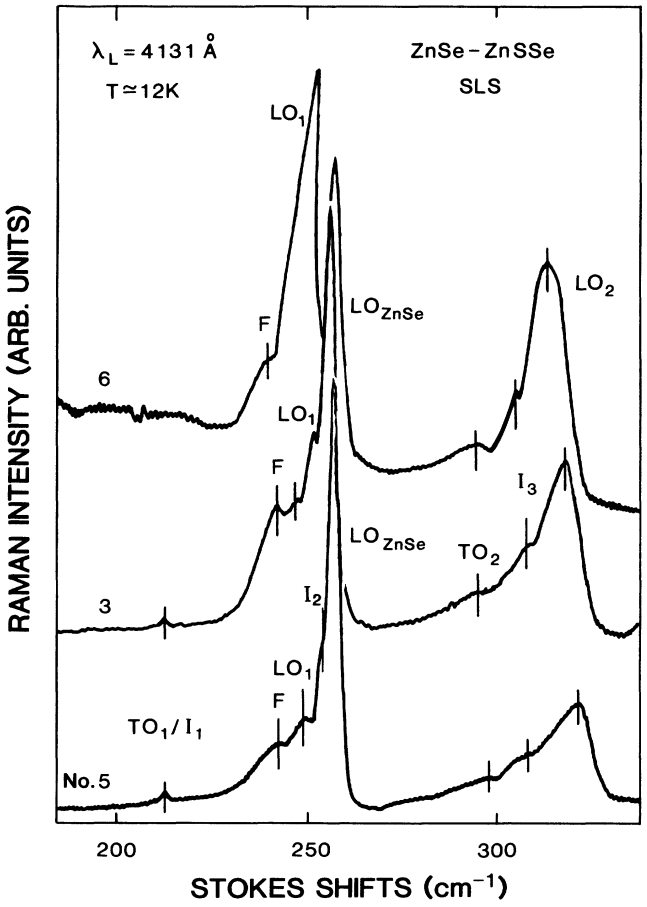

FIG. 5. First-order Raman spectra of ZnSe-ZnS_xSe_{1-x} strained-layer superlattices. The LO_{ZnSe} and LO_2 peaks are due to confined longitudinal-optical modes in the ZnSe and ZnS_xSe_{1-x} layers, respectively. The LO_1 and F peaks are attributed to delocalized optical phonons and the I_i bands to interface vibrations. The TO_i are the transverse-optical modes of the ternary layers.

the Fröhlich interaction-induced mechanism and the B_2 phonons through the dipole-allowed deformation potential one. The presence of the I_i and TO_i modes indicates some relaxation of $\mathbf{q}$ conservation in the scattering process, which is not unusual in resonance.[10] The depolarized spectra recorded in the configuration $z(x+y,x-y)\bar{z}$ yielded almost flat line shapes as expected from the selection rules. For comparison we also measured some samples in the configurations $z(x,x)\bar{z}$ (A_1 modes allowed) and $z(x,y)\bar{z}$ (B_2 modes allowed). The $z(x,x)\bar{z}$ spectra are very similar to the $z(x+y,x+y)\bar{z}$ ones. On the other hand, the intensities in the $z(x,y)\bar{z}$ case are weaker than in the polarized configurations with almost no scattering at the LO_{ZnSe} frequencies. We conclude that the LO_{ZnSe} peaks seen in Fig. 4 show predominantly a A_1 character and that A_1 and B_2 symmetries contribute to the other LO-like modes. Our results for the symmetry of the confined phonons excited in resonance in the ZnSe layers agree with similar observations reported for modes in binary slabs of other superlattice systems.[2,10]

We discuss next the dependence of the LO_{ZnSe} Raman peaks on d_{ZnSe} and D, from which information about confinement and strain will be obtained. We begin with the case of the thinnest superlattice (samples 1, 8, and 9) for which D is comparable and only d_{ZnSe} varies. Because these superlattices are so thin ($D \leq 0.15$ μm) they are expected to conform to the ZnSe buffer layers and therefore have strain-free ZnSe layers. Indeed, this assessment has been confirmed by photoluminescence and transmission-electron microscopy in the SLS 1. The energies of the photoluminescence bands due to recombinations in the ZnSe wells can be explained by considering only quantum-size effects in the electron and hole subbands without strain-induced shifts,[15] whereas the transmission-electron-microscopy investigations have unveiled almost dislocation free superlattice-buffer layer interfaces.[16] The spectra due to the LO_{ZnSe} modes of these samples are plotted in Fig. 6. We can see that the LO_{ZnSe} peaks appear at smaller frequencies than the undisturbed LO frequency of bulk ZnSe which is pointed out by the arrow, and that the shifts towards lower frequencies become more pronounced with decreasing d_{ZnSe}. The measured shifts with respect to the ZnSe bulk LO frequency (256.3 cm^{-1} at 12 K) are -1, -2.9, and -4.2 cm^{-1} for the SLS 1, 8, and 9, respectively. The trend in the negative shifts of LO_{ZnSe} with d_{ZnSe} is in qualitative agreement with the behavior depicted in Fig. 4 for confined modes in the ZnSe slabs of superlattices. Confined A_1 phonons are characterized by even n values.[1,10] Hence, we attribute the peaks seen in Fig. 6 as the $n=2$ confined modes in the ZnSe slabs with $\epsilon=0$. This interpretation is supported by the quantitative comparison between the measured and predicted negative shifts due to confinement. The experimental results are plotted in Fig. 4 and a very good agreement is obtained between the model and the experiment. For the shift of -4.2 cm^{-1} corresponding to sample 9 the equivalent q_n is ≈ 0.3 and therefore within the limits in which the measured $\omega(\mathbf{q})$ is well described by the theoretical expression discussed in Sec. IV. Confined modes with $n=4$ or larger are not observed because their predicted shifts are larger than or comparable

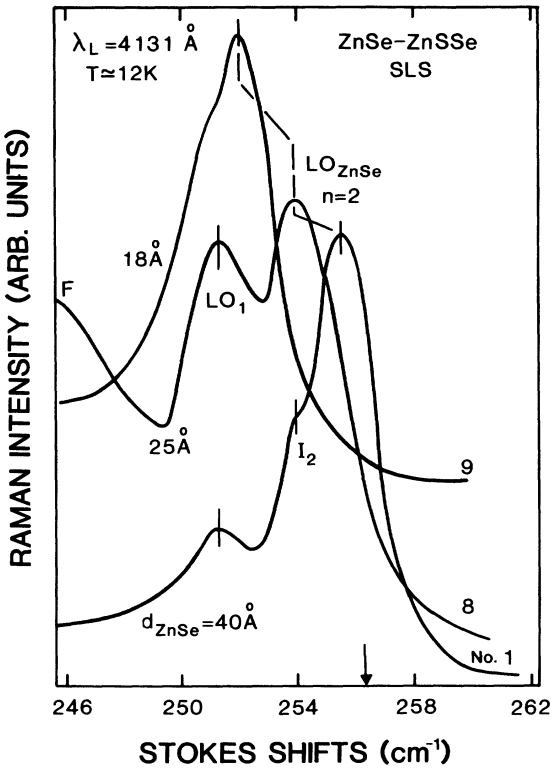

FIG. 6. Raman spectra of the superlattices with $D \leq 0.15$ μm for frequencies in the neighborhood of the longitudinal-optical modes of ZnSe. With decreasing ZnSe layer thickness d_{ZnSe} the LO_{ZnSe} peaks shift below the frequency value in the bulk, which is pointed out by the arrow. Because these superlattices conform to the ZnSe buffer layers, the LO_{ZnSe} shifts allow to determine confinement related effects. The LO_{ZnSe} peaks correspond to the $n=2$ confined modes of A_1 symmetry.

to the LO_{ZnSe}-LO_1 difference, and therefore they overlap with the continuum provided by the LO_1 vibrations.

We follow now the behavior of the $n=2$ modes when D changes and d_{ZnSe} is kept more or less constant (or better the ratio $d_{ZnSe}/d_{ZnS_xSe_{1-x}}$). In Fig. 7 the LO_{ZnSe} peaks are shown for the case of $d_{ZnSe} \approx 40$ Å and D ranging between 0.1 and 1 μm (samples 1–4). With increasing D the LO_{ZnSe} peaks move progressively from below the undisturbed bulk frequency in thinner superlattices ($D < 0.5$ μm) to values above it in the thicker samples ($D \geq 0.5$ μm). Concomitant with the shifts some broadening of the lines also takes place. The progressive shifts to higher energies are indicative of a buildup of compressive strain in the ZnSe layers. As D increases misfit dislocations are generated at the interfaces between the buffer layer and the superlattices. There is a loss of registry between both structures and the superlattices will try to relax to an equilibrium lattice constant of their own. Such lattice constant will be smaller than the bulk value of a_{ZnSe} thus compressively straining the ZnSe layers. The evolution of the peak positions with D shown by the spectra in Fig. 7 provides a clear demonstration of strain overcoming confinement in the determination of the optical frequencies. The measured shifts in the LO_{ZnSe} peak

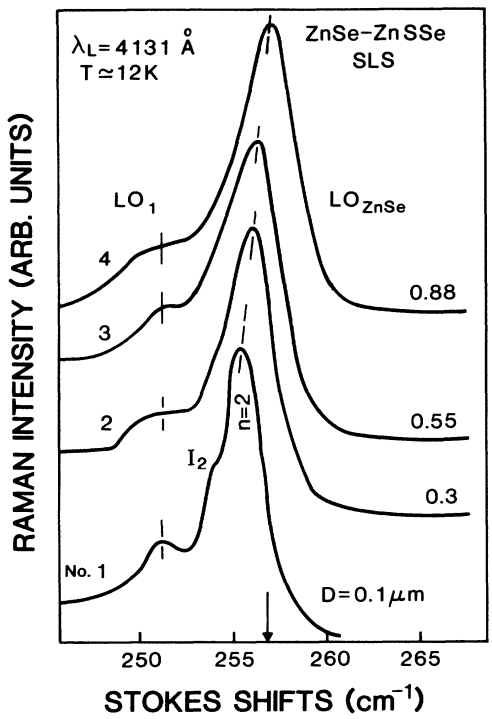

FIG. 7. Behavior of the $n=2$ LO_{ZnSe} peaks as a function of the superlattice thickness D for samples of comparable individual layer thicknesses. With increasing D the peaks shift from frequencies below the undisturbed value in the bulk, which is indicated by the arrow, to frequencies above it. The shifts are due to a progressive tetragonal distortion of the ZnSe unit cell induced by a biaxial compressive strain. The evolution of the peak positions exemplifies the situation of strain overcoming confinement in the frequency renormalization.

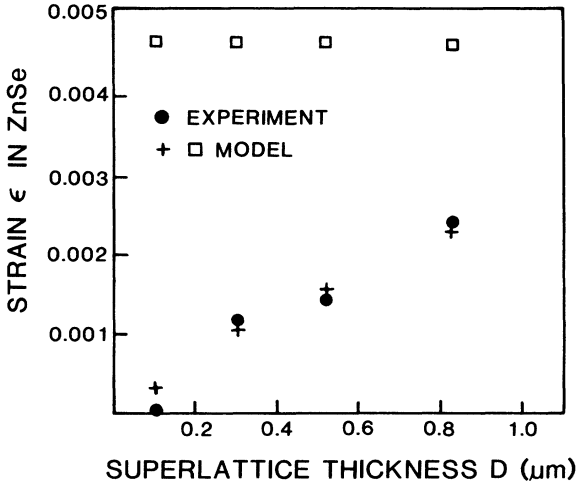

FIG. 8. Compressive strains in the ZnSe layers along the x and y directions, as a function of the total superlattice thickness D. The experimental values (solid dots) were determined from the LO_{ZnSe} shifts with respect to the value for the thinnest superlattice in the previous figure. The calculated strains represent the results of two limiting situations. The one that describes the experiment more closely (crosses) assumes that the superlattice-buffer layer is one structure. The other (squares) assumes that the superlattices are free standing. From these results, it is concluded that the transition from congruent to a free-standing state is continuous.

positions with respect to the value for sample 1 ($D=0.1$ μm; $\epsilon=0$) together with the relationship $\Delta\omega(\epsilon)$ given in the previous section were used to determine ϵ in the ZnSe layers. In Fig. 8 the solid dots represent the experimentally determined values of ϵ which are displayed as a function of D. A gradual increase of ϵ with D is realized.

Interesting to note is the fact that for $D \leq 1$ μm the experimental values of ϵ are much smaller than $f/2$ which is approximately the expected strain if the SLS were free standing.[17] That is if the equilibrium lattice constant were determined by the elastic properties and thicknesses of the slabs in the superlattice without any influence from the buffer layer. The squares in Fig. 8 give the calculated ϵ in the free-standing situation. By comparing the experimental and calculated ϵ in the free-standing case, it is concluded that the transition from a pseudomorphic state into a free-standing situation is not abrupt. This kind of conclusion about the nature of the transition was reached before in experiments carried on in the superlattice 6,[14] and was confirmed recently with photoluminescence spectroscopy.[18] The experimental ϵ are also compared to the predictions of the model which considers the buffer layer and superlattice as one entity. In addition to the slab thicknesses, the relative contributions of D and the buffer layer thickness are weighted in the calculation of the in-place equilibrium lattice constant for the whole structure. By applying the formalism given in Eqs. (5) and (6) of Ref. 2 we calculated the values of ϵ displayed as crosses in Fig. 8. The results yielded by this second approach describe the experiment more closely for the samples shown in Fig. 7 and for the other samples in Table I as well. Only at the top of superlattice 6 the measured strains achieve free-standing values. This is a very thick SLS and in its case both models predict similar ϵ. In the model that the superlattice plus buffer layer can be treated as one entity the role of the misfit dislocations is not included. The good agreement between the dots and the crosses in Fig. 8 seems to indicate that in first approximation this is the case at least for $D<0.8$ μm. It will be interesting to perform a similar study in other superlattices comprising group-IV elements and III-V compound semiconductors to ascertain if the continuous transition is a general property of SLS or if it is the case in II-VI superlattices because of the smaller elastic constants of these materials. The realization that strain can depend critically on D is relevant in the analysis of other properties of the SLS such as band offsets and nonlinear response. For II-VI heterostructures and superlattices theoretical models and experimental results suggest very small conduction- or valence-band discontinuities depending on the particular materials. Therefore, the final band lineup and type of the superlattice will be strongly determined by the magnitude of the strain at the interfaces and as we have shown this is not only a function of the individual layer thicknesses but also D.

We mentioned before that the LO_2 Raman peaks in

Fig. 5 are confined modes in the ZnS_xSe_{1-x} layers. In principle one can analyze these modes in similar fashion as it was done for LO_{ZnSe}. However, we can see in Fig. 5 that the linewidths of these peaks are at least a factor of 3 larger than for the LO_{ZnSe} case, which from an experimental point of view precludes the high-resolution spectroscopy needed to distinguish between confinement and strain. On the other hand, the frequency renormalization due to confinement is expected to be very small because of contributions of modes with $n=1$ (B_2 symmetry). Also, the estimated shifts due to strain (to lower frequencies for this mode) are on the order of the shifts that can be produced by any reasonable compositional fluctuation in the alloy layer (of about 2%). It is not surprising then, that the LO_2 frequencies depend more strongly on x than any other sample parameters. Therefore, we will not discuss this mode any further.

The Raman bands labeled I_i in Fig. 5 have been attributed to the interface modes and we will outline here the reasons leading to this assignment. Interface modes have been studied recently in binary-binary and binary-ternary superlattices and from these investigations some universal properties of the modes have been established.[1,8,9] One of the basic characteristics is of course their frequency. We have discussed in Sec. III in which spectral range the interface vibrations should be, for the case of ZnSe-ZnS_xSe_{1-x} superlattices with the parameters given in Table I. The measured frequencies of the I_i bands in Fig. 5 are $\approx$307, 253, and 211 cm^{-1} for I_3, I_2, and I_1, respectively. These frequencies are in the spans shown by the arrows in Fig. 2. The only ambiguity in the assignment can arise between I_1 and TO_1 because of the narrow range possible for the I_1 mode. Another attribute of the interface modes used in their characterizations is related to the fact that they display amplitude on both sides of the interface. Therefore, their Raman scattering cross section should have resonant enhancements at energy gaps of both layers of the superlattice.[8] This property of the I_i modes has been confirmed by monitoring their behavior in multiphonon scattering. The results are presented in Fig. 9 for SLS 3 and 6. The new information reported in this figure relates to the Raman structures observed in the range between 400 and 900 cm^{-1}. They correspond to overtone combinations by some of the $q\approx 0$ modes seen in the first-order spectra between 200 and 320 cm^{-1}. The identification of the overtones was done based on the measured first-order frequencies. The agreement between the peak positions and the added frequencies is better than 1 cm^{-1} in most of the cases. We can see that the I_i modes pair exclusively among each other in qualitative agreement with similar behavior reported in other heterostructures.[2,19,20] In both spectra displayed in Fig. 9, the overtone Raman lines are on the top of broad photoluminescence backgrounds thus giving resonant conditions with the outgoing channel.[6] In sample 6 the luminescence is due to radiative transitions across the E_0 gap of the ternary layers at 2.91 eV (apparent Stoke shift of 750 cm^{-1} with respect to the 4131-Å laser line). The combined effects of a smaller d_{ZnSe} and larger x in sample 3 as compared with sample 6 produce a shift of E_0 and of the fundamental gap of the superlattice in the ZnSe layers to higher energies (to the left in the way the spectra are plotted in Fig. 9). As a consequence, the luminescence background is now given by the high-energy tail of the recombination spectra taking place across the fundamental gap of the superlattice in the ZnSe layers. This gap is at $\approx$2.83 eV and its photoluminescence peak has a Stoke shift of about 1400 cm^{-1} when excited with the 4131-Å line. The striking feature of the data in Fig. 9 and at the same time reassuring of the identification made is that the overtones due to the I_i modes appear in resonance with the gaps in ZnSe and in ZnS_xSe_{1-x}, whereas, for example, the LO_i modes resonate only with the gap in ZnS_xSe_{1-x}. We note that in sample 3 no overtones of the LO_{ZnSe} modes are observed. One of the reasons for their absence is that the scattered photon energies do not overlap exactly with the gap energy as is the case for sample 6. The observation of the interface modes implies a breakdown of wave-vector conservation due to imperfection at the interfaces. The use of these modes in the characterization of the quality of the ZnSe-ZnS_xSe_{1-x} interfaces will be pursued in a forthcoming publication.

In the final part of the discussion we would like to refer to the peaks labeled F in Fig. 5. A blowup of the spectral

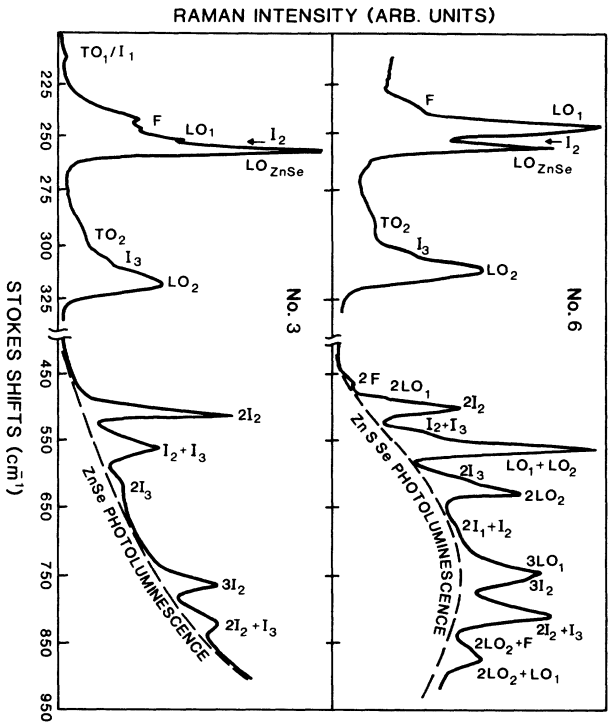

FIG. 9. Comparison between the overtone spectra (450–900 cm^{-1}) of superlattices 3 and 6 to determine the resonant response of the interface modes I_i to excitation energies close to gaps in both layers of the superlattice. The spectra show that the I_i modes combine among themselves and that their overtones resonate with ZnSe and ZnS_xSe_{1-x} gaps. This behavior reaffirms the assignment of the nature of the I_i Raman bands seen in the first-order part of the spectra (200–330 cm^{-1}).

range in which these Raman bands are seen is presented in Fig. 10 for samples with different periods d. The spectra displayed in this figure point out that the F bands appear as the superlattice period d decreases below ≈ 120 Å. We have not been able to establish a trend of the frequency of these bands on d because they show up as broad structures. In general they peak in the neighborhood of 240–245 cm^{-1} and have linewidths of at least 10 cm^{-1}. However, in some samples two structures can be distinguished and labeled F. As an example, the spectra shown in Figs. 5 and 10 for SLS 3 display a second F band peaking just below LO_1.

The appearance of the F bands in the superlattice data is indeed intriguing. We mentioned in Sec. III that scattering at these frequencies is not observed in the spectra of ternary alloys shown in Fig. 1, from which we conclude that the F peaks have to be related with some effect taking place in the superlattices or being induced by the extra periodicity. We cannot explain these peaks by assuming that in the superlattices zone-edge modes become Raman active. There is no correlation between the zone-edge frequencies of ZnSe and ZnS and the frequencies of the F modes.[11,21] Along the same lines second-order scattering by acoustic modes cannot be invoked because it has not been observed in ZnSe or ZnS at these frequencies.[22] Also, second-order scattering by acoustic phonons in II-VI semiconductors is observed only with laser light below the absorption edge.[6] When the SLS are excited with the 5145-Å line of an argon laser, the F bands do not show up. Finally, the possibility of severely distorted and therefore graded interfaces can also be ruled out. If the F bands were to represent the LO_1 mode of a graded region near the interfaces, then the LO_2 counterpart at around 330 cm^{-1} should be observed. This is clearly not the case even though we diligently searched for such mode. In addition other studies done with photoluminescence, x-ray diffraction, and transmission-electron microscopy do not support the notion of interfacial regions extending over several lattice constants. Having ruled out these alternatives that under certain circumstances can arise in superlattices, we tentatively identified the F modes as due to scattering by folded or delocalized optical modes. Such modes will have frequencies in the range in which the LO vibrations of both layers overlap and can propagate throughout the entire superlattice.[1,12]

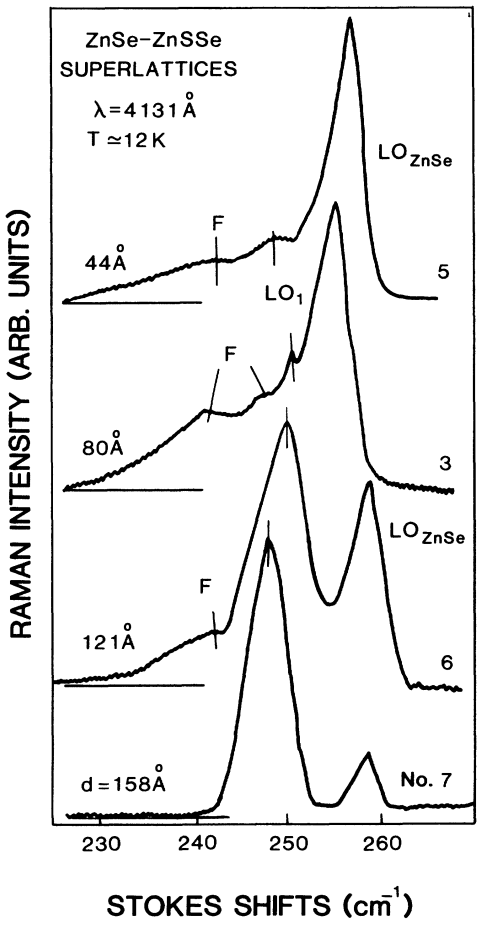

FIG. 10. Stokes Raman spectra in the neighborhood of the so-called F bands displayed as a function of the superlattice period d. The horizontal solid lines indicate the background level in each spectrum. The F structures appear as d decreases below ≈ 120 Å. They are assigned to delocalized optical phonons. The stronger intensities of the LO_1 peaks in the spectra of samples 6 and 7 are due to a closer resonance with the ternary gap and to a much thicker ternary layer, respectively.

Folding of the LO dispersion $\omega(\mathbf{q})$ will produce numerous branches in a relatively narrow range of frequencies because of its weak quadratic dependence on $\mathbf{q}$. This situation is illustrated in Fig. 11 in which the $\omega(q)$ dispersion described in Sec. IV has been folded in a zone whose edge is given by $na/2d$ (in units of $2\pi/a$). We have chosen the parameters of sample 3 and the value of LO_1 as $\omega(0)$ and made no distinction in the lattice parameters a of ZnSe and ZnS_xSe_{1-x}. Note that d is being used instead of d_i in determining the zone edge.[10] The arrow indicates the momentum transfer in the scattering process given by $4\pi n_{RI}/\lambda_{laser}$ where n_{RI} is the refractive index of ZnSe at $\lambda_{laser}=4131$ Å.[5,6] When the folded dispersion is compared to the measured spectra, there is agreement in the overall frequency range of the folded branches and the experimental F bands. However, we cannot make a definite assignment of the order n of the modes being observed. This was not expected anyway because of the simplicity of the model. In the framework of our interpretation of the nature of the F bands, they correspond to weighted scattering from several of the folded branches. As d increases the folded branches become very close to each other and form a continuum of frequencies below LO_1. This can explain why the F Raman bands are not seen in the larger period SLS. Recently the lattice-dynamic properties of $GaAs\text{-}Ga_{1-x}Al_xAs$ superlattices have been studied theoretically and low-frequency sidebands in the Raman spectra of the confined optical modes have been predicted because of the folded optical ones.[23] The observation of the F bands in our superlattices is very much in line with this theoretical prediction.

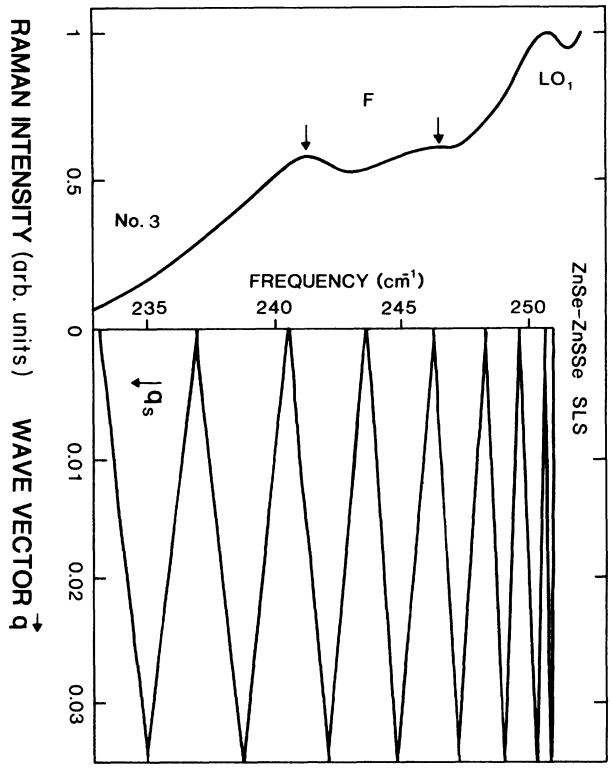

FIG. 11. Comparison between frequency ranges of the F bands in the Raman spectra and of the folded branches of the $\omega(q)$ dispersion shown in Fig. 3 and discussed in Sec. IV. The minizone edge corresponds to the period of SLS 3. The arrow indicates the momentum transfer in the scattering process. The F bands are interpreted as weighted scattering from several folded branches.

In the overtone spectra of sample 6 in Fig. 9, the F peaks are seen to participate in multiphonon processes in resonance with the ZnS_xSe_{1-x} gap. Unfortunately, overtones of the F bands are not observed in resonance with the ZnSe gap in the spectra of sample 3. As for the I_i modes, the folded optical phonons should resonate with gaps in both layers of the superlattice. Their absence from the multiphonon spectra of sample 3 can be due to the same reasons that preclude the observation of LO_{ZnSe} overtones. Additional experimental work with superlattices of larger x in the ternary layers, thus given a larger gap between LO_{ZnSe} and LO_1 and more variation in the ratios $d_{ZnSe}/d_{ZnS_xSe_{1-x}}$ is expected to yield additional information on the nature of the F bands.

VI. CONCLUSIONS

ZnSe-ZnS_xSe_{1-x} strained-layer superlattices display very rich Raman spectra from which we were able to study some of the lattice dynamic properties of these structures. We established that the phonon frequencies and nature of the modes are determined by superlattice effects produced by the successive stacking of ZnSe and ZnS_xSe_{1-x} layers and by interfacial strains due to the different lattice constants of these semiconductors. We succeeded in differentiating both phenomena by careful selection of sample parameters. To guide the analysis of the superlattice Raman spectra we also presented data on the vibrational properties of ZnS_xSe_{1-x} ternary alloys. Some of the peaks observed in the superlattices spectra were readily identified as due to confined optical modes and interface phonons. Other peaks were tentatively assigned to delocalized or folded optical modes. It was shown that the frequencies of the LO modes confined in the ZnSe layers depend on the layer thickness d_{ZnSe} and the total superlattice thickness D. The dependence of the frequencies on d_{ZnSe} revealed the effect of confinement and that on D the influence of strain. The frequency renormalization due to these effects has opposite signs. In the absence of strain, the shifts due to confinement are well described with the bulk phonon dispersion and the appropriate relationship between the wave vector and d_{ZnSe}. From the strain-induced shifts, it was possible to study the nature of the transition from the state in which the superlattices conform to the buffer layer to the free-standing cases in which they have a lattice constant of their own. We determined that this transition takes place gradually. The interface modes appear in the frequency ranges predicted by the theoretical models, namely, where the ratio of the dielectric constants is negative. Their overtone spectra exemplify very nicely the property of resonant enhancement with energy gaps of both layers of the superlattices. The peaks interpreted as folded optical modes are seen in superlattices of relatively short periods. Their assignment was based on the fact that they appear at frequencies for which a strong overlap takes place between the ZnSe and ZnS_xSe_{1-x} vibrations. They participate in overtone scattering in combination with other longitudinal-optical modes. Future experiments were suggested to characterize them in more detail.

ACKNOWLEDGMENTS

We would like to acknowledge discussions with J. Petruzzello and the communication of his transmission-electron-microscopy results previous to publication. The help of R. Dalby in the growth of the superlattices is gratefully acknowledged.

*Present address: Philips Research Laboratories, P.O. Box 80 000 NL-5600 JA Eindhoven, The Netherlands.

[1]A recent review on the subject with a comprehensive list of references has been published by M. V. Klein, IEEE J. Quantum. Electron. **QE-22**, 1760 (1986), and references therein. See also, S. Ren, H. Chu, and Y. Chang, Phys. Rev. Lett. **59**, 1841 (1987); E. Richter and D. Strauch, Solid State Commun. **64**, 867 (1987).

[2]E. K. Suh, D. U. Bartholomew, A. K. Ramdas, S. Rodiguez, S. Venugopalan, L. A. Kolodziejski, and R. L. Gunshor, Phys. Rev. B **36**, 4316 (1987).

[3]S. Nakashima, Y. Nakakura, H. Fujiyasu, and K. Mochizuki, Appl. Phys. Lett. **48**, 2366 (1986); S. Nakashima, A. Wada, H. Fujiyasu, M. Aoki, and H. Yang, J. Appl. Phys. **62**, 2009 (1987); M. Kobayashi, M. Konagai, K. Takahashi, and K. Urabe, *ibid.* **61**, 1015 (1987).

[4]K. Mohammed, D. A. Cammack, R. Dalby, P. Newbury, B. L. Greenberg, J. Petruzzello, and R. N. Bhargava, Appl. Phys. Lett. **50**, 37 (1987).

[5]See, for example, H. Hartmann, R. Mach, and B. Selle, in *Current Topics in Material Science,* edited by E. Kaldis (North-Holland, Amsterdam, 1982), Vol. 9, p. 1.

[6]M. Cardona, in *Light Scattering in Solids II,* edited by M. Cardona and G. Güntherodt (Springer, Heidelberg, 1982), p. 9.

[7]O. Brafman, I. F. Chang, G. Lengyel, S. S. Mitra, and E. Carnall, Phys. Rev. Lett. **19**, 1120 (1967).

[8]A. K. Sood, J. Menendez, M. Cardona, and K. Ploog, Phys. Rev. Lett. **54**, 2115 (1985).

[9]A. K. Arora, A. K. Ramdas, M. R. Melloch, and N. Otsuka, Phys. Rev. B **36**, 1021 (1987).

[10]A. K. Sood, J. Menendez, M. Cardona, and K. Ploog, Phys. Rev. Lett. **54**, 2111 (1985); **56**, 1753 (1986); B. Jusserand and D. Paquet, *ibid.* **56**, 1752 (1986).

[11]B. Hennion, F. Mousa, G. Pepy, and K. Kunc, Phys. Lett. **36A**, 376 (1971).

[12]B. Jusserand, D. Paquet, and A. Regreny, Phys. Rev. **30**, 6245 (1984).

[13]F. Cerdeira, C. J. Buchenauer, F. H. Pollak, and M. Cardona, Phys. Rev. B **5**, 580 (1972).

[14]D. J. Olego, K. Shahzad, J. Petruzzello, and D. A. Cammack, Phys. Rev. B **36**, 7674 (1987).

[15]K. Shahzad, D. J. Olego, and C. Van de Walle, Phys. Rev. B **38**, 1417 (1988).

[16]J. Petruzzello, O. Boser, and P. Kellawon, *Defects in Electronic Materials, Material Research Society Symposium 104, Boston, 1987,* edited by M. Stavola, S. J. Pearton, and G. Davies (Materials Research Society, Pittsburgh, 1988), p. 629.

[17]G. C. Osbourn, J. Appl. Phys. **53**, 1586 (1981).

[18]K. Shahzad, D. J. Olego, and D. A. Cammack, Appl. Phys. Lett. **52**, 1416 (1988).

[19]A. K. Sood, J. Menendez, M. Cardona, and K. Ploog, Phys. Rev. B **32**, 1412 (1985).

[20]M. H. Meynadier, E. Finkman, M. D. Sturge, J. M. Worlock, and M. C. Tamargo, Phys. Rev. B **35**, 2517 (1987).

[21]N. Vagelatos, D. Wehe, and J. S. King, J. Chem. Phys. **60**, 3613 (1979).

[22]R. L. Schmidt, K. Kunc, M. Cardona, and H. Bilz, Phys. Rev. B **20**, 3345 (1979).

[23]A. Kobayashi and A. Roy, Phys. Rev. B **35**, 2237 (1987).